manuscripta geodaetica (1995) 20:161–172

manuscripta geodaetica

© Springer-Verlag 1995

Application of the wavelet transform for GPS cycle slip correction and comparison with Kalman filter

F. Collin and R. Warnant

Royal Observatory of Belgium, Avenue Circulaire 3, B-1180 Brussels, Belgium

Received 23 November 1992; Accepted 4 January 1995

Abstract

In the past, several authors introduced a method based on phase and/or code combinations of GPS data together with a Kalman filter to solve the problem of the cycle slips. In this paper, the same philosophy is used but a comparison of the results obtained with Kalman filtering and the wavelet transform is performed. The wavelet transform is a rather new spectral analysis method which is introduced in the second paragraph. The comparison of the two methods is accomplished in several steps: first, some data points are removed and jumps are simulated in theorical and real signals to test the capability of the wavelet transform to model the signal i.e. to recover the removed data points and to compute the value of the jumps. Then, the analysis is performed on real cycle slips. This last study shows that the wavelet transform and the Kalman filter are very complementary and give both correct values for the cycle slips.

1 GPS cycle slip problem and Kalman filter

1.1 Introduction

The P-Code dual frequency GPS receivers can perform two types of measurements:

- Pseudorange (P-Code) measurements $P_i(t)$ with:

$$\begin{aligned} P_i(t) &= c\ \Delta t_i(t) \\ &= \rho(t) + I_i(t) + T(t) + c(\delta^S(t) - \delta^R(t)) \end{aligned}$$

where

  - δ^S is the satellite clock error
  - δ^R is the receiver clock error
  - $i = 1, 2$ refers to the carrier L1 or L2
  - t is the time of the pseudorange measurement
  - c is the speed of light
  - Δt_i is the code signal time of transit from satellite to receiver
  - ρ is the geometrical distance between the position of the satellite at time of emission of the GPS signal and the receiver at time t
  - I_i is the frequency dependent path lengthening due to ionospheric refraction
  - T is the frequency independent path lengthening due to tropospheric refraction

- carrier beat phase measurements $\Phi_i(t)$:

$$\begin{aligned} \Phi_i(t) &= {}_r\Phi_i^S(t) - \Phi_i^R(t) + N_i \\ &= -\left(\frac{f_i}{c}\right)(\rho(t) - I_i(t) + T(t)) \\ &\quad + f_i(\delta^R(t) - \delta^S(t)) + N_i \end{aligned}$$

where

  - ${}_r\Phi_i^S$ is the phase of the L_i carrier received from the GPS satellite by the GPS receiver
  - Φ_i^R is the phase of the L_i reference signal generated by the receiver
  - N_i is the unknown integer ambiguity inherent in the GPS phase observations
  - f_i is the nominal L_i carrier frequency

This mathematical model of the GPS observables is very simple: it is valid under the assumption that the receiver and satellite reference frequencies are constant with time. Accepting this assumption does not affect the results of this paper. A more complete model can be found in King et al.(1987).

GPS receivers continuously monitor the carrier beat phase Φ_i. When they lose lock on a satellite, an unknown integer number of cycles is lost. This event is called a 'cycle slip'. These cycle slips have to be recovered in order to compute accurate positions.

The first step in the cycle slip correction consists in setting up a test quantity which is a combination of code and/or phase measurements. This combination has to be a slowly time varying function so that a jump in this function will indicate the occurrence of a cycle slip.

A first approximation of the cycle slip is computed using two phase-code combinations PC_i (units of cycles):

$$\begin{aligned} PC_i(t) &= (\Phi_i(t) + \left(\frac{f_i}{c}\right) P_i(t)) \\ &\quad -(\Phi_i(t_0) + \left(\frac{f_i}{c}\right) P_i(t_0)) \\ &= 2\left(\frac{f_i}{c}\right)(I_i(t) - I_i(t_0)) \end{aligned}$$

where t_0 is the time of the first measurement.
This function describes the evolution of the ionospheric refraction effect since the first measurement. If a cycle slip of ΔN_i cycles occurs, it will give rise to a jump ΔN_i in the beat phase Φ_i but not in the pseudorange P_i. As a consequence, this cycle slip will result in a jump ΔN_i in the phase-code combination PC_i. When such a jump has been detected, a first approximation of the cycle slip can be computed using the fact that ΔN_i has to be an integer number. Unfortunately, the noise level of the pseudorange measurement obtained with the best P-Code receivers is of the order of one L_i cycle for elevations above 45 degrees. Larger values (5 to 10 cycles) are observed in the case of multipath, Anti-Spoofing, and for low elevations. As a consequence, this method only gives a first approximation of the jump.

The final correction is obtained by using a L_1/L_2 combination PP:

$$\begin{aligned} PP &= \Phi_1 - \left(\frac{f_1}{f_2}\right)\Phi_2 \\ &= \left(\frac{f_1}{c}\right)(I_1(t) - I_2(t)) + N_1 - \left(\frac{f_1}{f_2}\right)N_2 \end{aligned}$$

It can be easily seen that the occurrence of a cycle slip (ΔN_1, ΔN_2) will give a jump ΔPP in the L_1/L_2 combination:

$$\Delta PP = \Delta N_1 - \left(\frac{f_1}{f_2}\right)\Delta N_2 \qquad (1)$$

The precision of the carrier beat phase measurements (Φ_1) is of the order of a few millimeters. This means that the resolution of this method is much better than the previous one. The disadvantage of equation (1) lies in the fact that it contains two unknowns ΔN_1, ΔN_2. Theorically this equation can be solved by using the first approximation given by the phase/code combination. In practice, a disturbed ionosphere, a low elevation angle, the multipath effect can seriously degrade the usefullness of this method. A more complete description can be found in (Bastos and Landau, 1988; Landau, 1989; Lichtenegger and Hoffmann-Wellenhof, 1989).

1.2 Kalman Filtering

In fact, in order to be able to detect a jump, we have to compare a predicted value of PP (or PC_i) with an observed one. Hence we need a mathematical method to model the evolution of PP (or PC_i) versus time.

The above mentioned authors make use of the following discrete Kalman filter (details in Gelb, 1974; Bastos and Landau, 1988):
System and measurement models:

$$\begin{aligned} \underline{X}_k &= \underline{\phi}_{k-1}\underline{X}_{k-1} + \underline{W}_{k-1} \\ \underline{Z}_k &= \underline{H}_k\underline{X}_k + \underline{V}_k \end{aligned}$$

State and error covariance prediction:

$$\begin{aligned} \underline{X}_k(-) &= \underline{\phi}_{k-1}\underline{X}_{k-1}(+) \\ \underline{P}_k(-) &= \underline{\phi}_{k-1}P_{k-1}(+)\underline{\phi}_{k-1}^T + \underline{Q}_{k-1} \end{aligned}$$

State and error covariance update:

$$\begin{aligned} \underline{X}_k(+) &= \underline{X}_k(-) + \underline{K}_k[\underline{Z}_k - \underline{H}_k\underline{X}_k(-)] \\ \underline{P}_k(+) &= [\underline{I} - \underline{K}_k\underline{H}_k]\underline{P}_k(-) \\ \underline{K}_k &= \underline{P}_k(-)\underline{H}_k^T\left[\underline{H}_k\underline{P}_k(-)\underline{H}_k^T + \underline{R}_k\right]^{-1} \end{aligned}$$

with :

$\underline{X}_k$ the state vector
$\underline{\phi}_k$ the transition matrix
$\underline{W}_k$ the state prediction error
$\underline{H}_k$ the matrix forming the observation equations
$\underline{P}_k$ the covariance of the state vector
$\underline{Z}_k$ the vector of observations
$\underline{V}_k$ the measurement error
$\underline{I}$ the identity matrix

$\underline{K}_k$ the Kalman gain matrix
$\underline{Q}_k$ the state transition noise matrix
$\underline{R}_k$ the covariance matrix of observations

The state transition model and the state transition covariance matrices are taken from Bastos and Landau (1988):

$$\underline{X} = \begin{bmatrix} y \\ \dot{y} \\ \ddot{y} \end{bmatrix} \text{ and } \underline{\phi} = \begin{bmatrix} 1 & \Delta t & \frac{\Delta t^2}{2} \\ 0 & 1 & \Delta t \\ 0 & 0 & 1 \end{bmatrix}$$

with Δt, the sampling rate, y, $\dot{y}$, $\ddot{y}$ the considered combination (PC_i or PP) and its derivatives.
Phase/Code combination:

$$Q = \begin{bmatrix} 10^{-8} & 0 & 0 \\ 0 & 10^{-10} & 0 \\ 0 & 0 & 10^{-12} \end{bmatrix} \begin{bmatrix} m \\ - \\ m^{-2} \end{bmatrix}$$

We use the elevation dependent measurement noise model given by Eueler and Goad (1991) for a Rogue Receiver :

$$R(m^2) = 0.08 + 4.5e^{-\frac{h}{10}}$$

where h is the elevation angle.
Phase combination:

$$Q = \begin{bmatrix} 10^{-6} & 0 & 0 \\ 0 & 10^{-8} & 0 \\ 0 & 0 & 10^{-10} \end{bmatrix} \begin{bmatrix} cycles^2 \\ - \\ cycles^{-2} \end{bmatrix}$$

$$R(cycles^2) = 5\,10^{-4}$$

In the next section, we will compare the results obtained by using this Kalman filter and the wavelet transform.

2 Introduction to the wavelet transform

The wavelet transform is born 6 years ago when scientists realized that the Fourier transform didn't answer all the questions about the frequency analysis.

To detect the frequencies present in a signal, Fourier projects this signal on trigonometric functions (sine and cosine) and their harmonics.

With the same goal, the wavelet transform projects the signal on a family of functions (named wavelets and noted $g_{ab}(t)$) issued from a basic function (noted $g(t)$) by dilatation (of factor 'a', called the scale) and translation (of factor 'b', called the time parameter). Formally the relation between $g_{ab}(t)$ and $g(t)$ is : $g_{ab}(t) = g(\frac{t-b}{a})$.

Figure 1 shows how the parameters 'a' and 'b' act on the basic wavelet.

When 'a' raises the wavelet stretches itself: the analysed part of the signal is larger and the wavelet essentially searches for the low frequencies. When 'a' decreases the wavelet contracts itself and a smaller part of the signal is considered. In this case the wavelet detects the high frequencies present in the signal.

The parameter 'b' shifts the wavelet over all the signal; this corresponds to a translation in time.

The coefficients of the wavelet transform $S(a,b)$ of a signal $s(t)$ are given by :

$$S(a,b) = \int g_{ab}(t).s(t)dt \qquad (2)$$

Generally the wavelet transform is a complex function of 'a' and 'b'. Therefore the information about the signal is included in the modulus and in the phase of the wavelet transform.

The use of the wavelet transform can be summarized as follows: a basic wavelet ($g(t)$) is choosen, it is dilated of a factor 'a' and translated of a factor 'b' ($g_{ab}(t)$) (see Figure 1). Then using equation (2), the signal is projected on $g_{ab}(t)$ giving the result $S(a,b)$. We make this operation for all the values of 'b' (shifting the wavelet over all the signal) and for all the values of 'a' (searching for all the frequencies) to obtain the wavelet transform of the signal.

While Fourier only gives the frequency composition of a signal with the assumption that all the component frequencies are present from the origin to the end of the 'infinite' signal, the wavelet transform gives the time location of each frequency, it allows the visualisation of transient frequencies, the analysis of the law of dispersion and the determination of the occurrence of discontinuities in a signal.

This new method of analysis has been applied to a wide range of physical problems: Nuclear Magnetic Resonance spectroscopy (Martens, 1989; Guillemain et al.,1989), synthesis of audio-sounds (Guillemain et al., 1991), galaxy counts (Slezat et al., 1990), study of multifractals (Arnéodo et al., 1988), astronomy (Bijaoui et al., 1991) and many more.

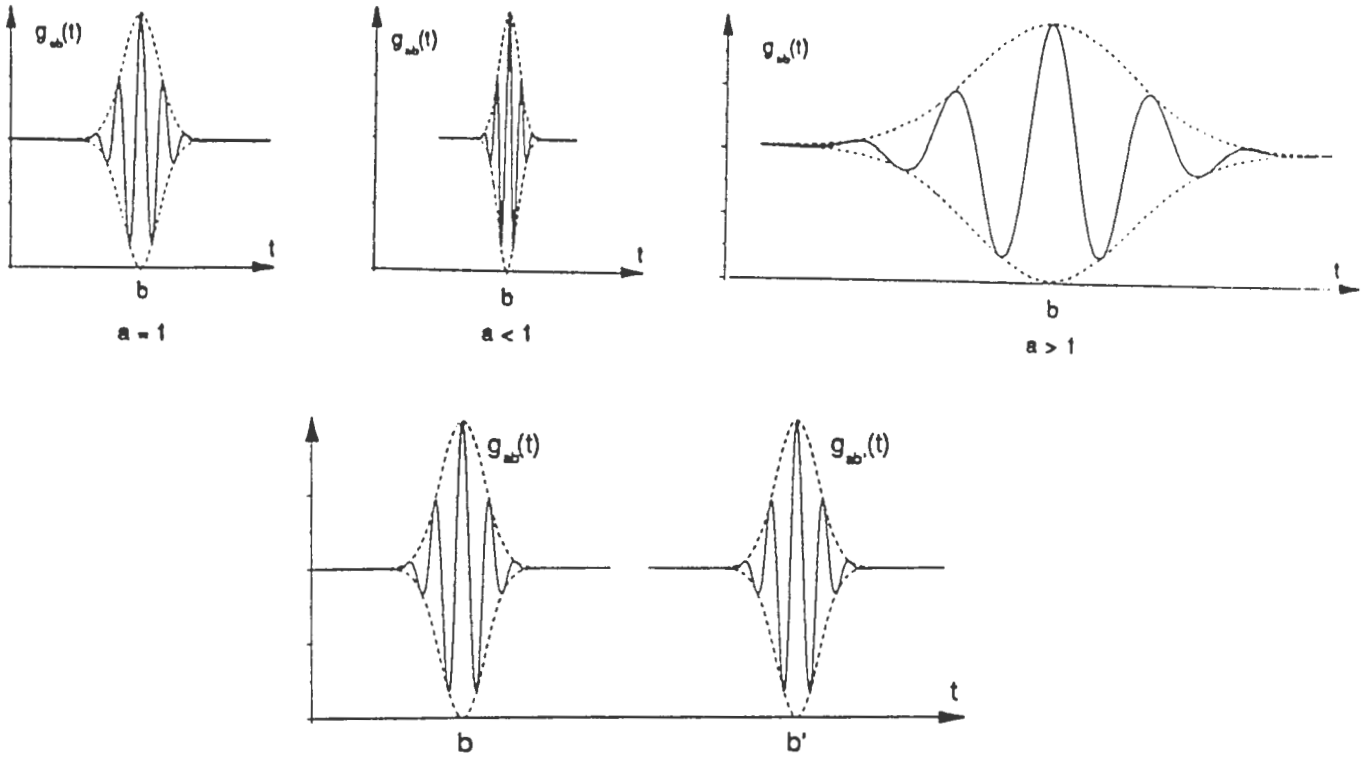

Figure 1: How 'a' and 'b' act on the wavelet

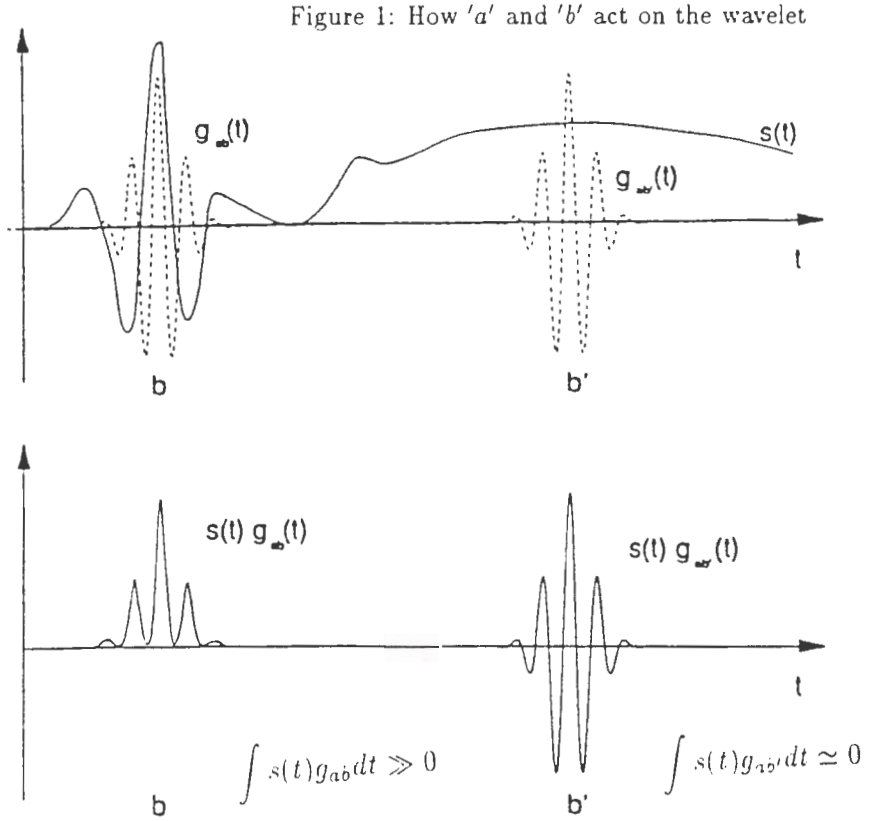

Figure 2: Effect of time-scale filter of the wavelets. In the first part of figure 2, a signal $s(t)$ is represented. The dashed line shows a wavelet for $t = b$ and $t = b'$. The second part of figure 2 displays the wavelet transform $S(a, b)$ of the signal $s(t)$ for $t = b$ and $t = b'$.

2.1 Properties of the wavelet transform

For simplicity, the following properties are given without any complicated mathematical demonstration. The evolution from the Fourier transform to the wavelet transform and the mathematical justifications of the wavelet transform can be found by the readers in Daubechies (1992), Chui (1991), Combes (1988), Meyer (1992), Grossman et al. (1992).

2.1.1 Zero mean of the wavelet

The wavelet must have zero mean, so that the projection of a signal dissimilar to the wavelet is almost zero ($\mid S(a,b) \mid \simeq 0$) and the projection of a signal similar to the wavelet has a large amplitude ($\mid S(a,b) \mid >> 0$).

This is an effect of the time-scale filter: the wavelet ($g_{a\,b}(t)$) only sees that part of the signal which it resembles (Figure 2).

The wavelet used to detect the cycle slips is built from this idea. The Doppler effect present in the GPS observations (due to the fact that the satellite is moving with respect to the receiver) leads to a parabolic walk of the signal. We will build the wavelet so that it will "see" the discontinuities in the GPS signal but not this second order walk.

2.1.2 Wavelet transform of a signal with a discontinuity

Figure 6 shows the shape of the wavelet transform of a signal $s(t)$ with a discontinuity in $t = 50$ as presented in Figure 3.

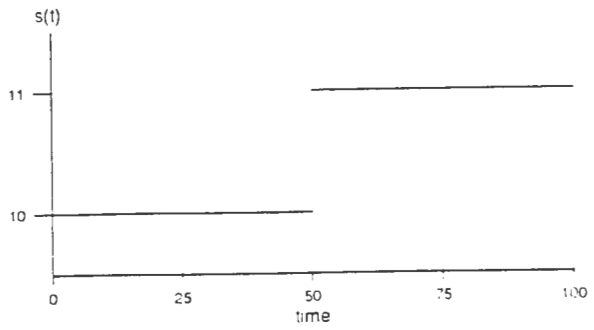

Figure 3: Signal with a discontinuity in $t = 50$

It appears that:
The modulus of the wavelet transform is maximum near the discontinuity, Grossman et al., (1992).

The basic idea of this work is based on this behaviour of the modulus near a discontinuity. Indeed, when this kind of behaviour is observed in the wavelet transform of a signal, the presence of a discontinuity will be deduced.

3 Cycle slip detection using the wavelet transform

3.1 Construction of the appropriate wavelet

Owing to the fact that the wavelet detects only parts of the signal similar to itself, a wavelet which looks like the discontinuities encountered in the GPS observations was built (Figure 4). Figure 7 shows such a discontinuity in the phase combination PP.

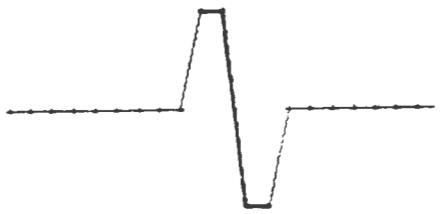

Figure 4: Original Wavelet

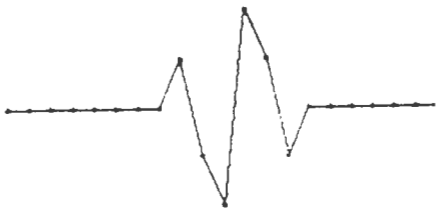

Figure 5: Final Wavelet

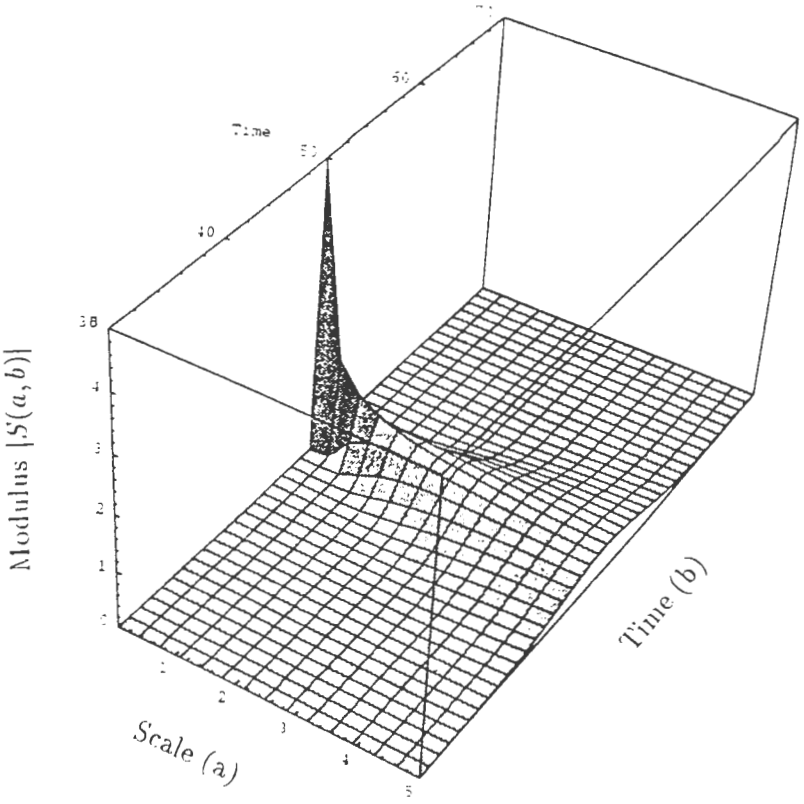

Figure 6: Modulus of the wavelet transform $|S(a,b)|$ of a signal $s(t)$ with a discontinuity in $t = 50$. $|S(a,b)|$ grows for $a \to 0$ and as a function of b: $|S(a,b)|$ is maximum near the discontinuity.

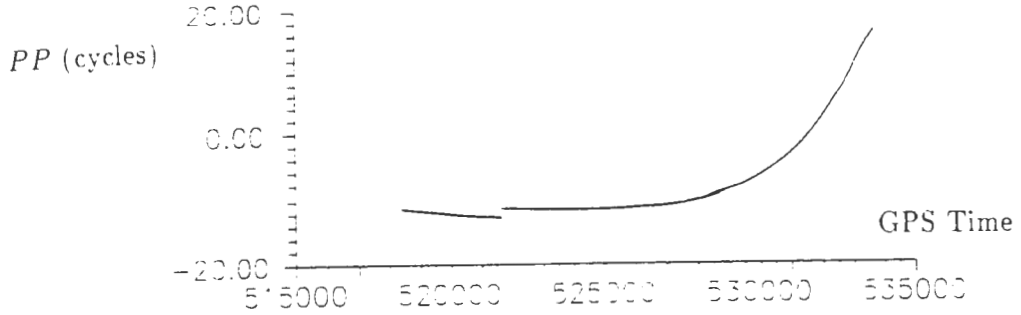

Figure 7: Cycle slip in the PP Combination

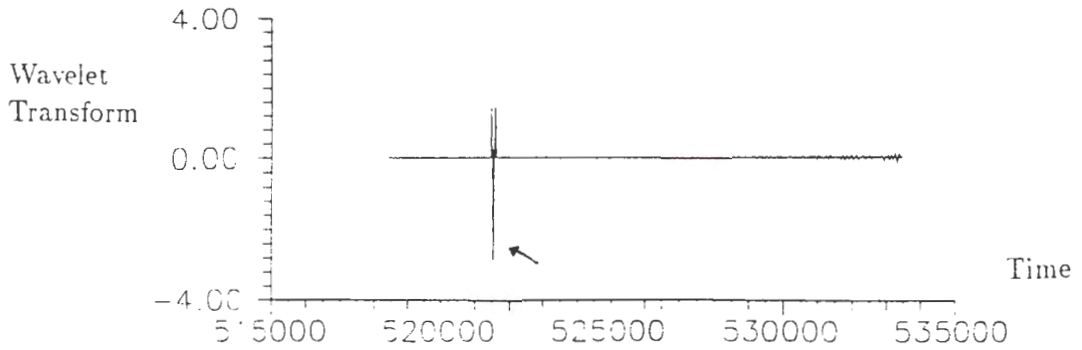

Figure 8: Modulus of the Wavelet transform of the signal displayed in figure 7. The occurrence of a cycle slip is indicated by the presence of 3 outliers.

This original wavelet was adapted in order to eliminate the artefacts introduced in the wavelet transform by the parabolic behaviour of the signal (as mentioned before). Indeed, the GPS carrier beat phase has a parabolic behaviour due to the Doppler effect. The original Wavelet was built to detect jumps versus an horizontal right line. The parabolic behaviour of the signal is "seen" by the Wavelet as a succession of jumps. The Wavelet to be used will detect jumps versus a parabola. The final Wavelet (Figure 5) has been obtained by deriving the original wavelet in order to remove the parabolic behaviour of the GPS signal. This wavelet is real: all the information will be contained in the amplitude of the transform.

To detect a discontinuity in the signal, it is sufficient to compute the wavelet transform of this signal for one value of the parameter "a" near zero. Indeed, Figure 6 shows that the module of the wavelet transform is maximum near $a = 0$ when a discontinuity appears in the signal.

This wavelet transform is reduced to the convolution product between the signal and the chosen wavelet.
Finally, in this case, the wavelet transform moves to the application of a discrete filter to the signal.

Mathematical formulation:

Given $X = \{x_i\}$, $i = 0.....N$ a signal with a discontinuity and given the filter F_b defined by the coefficients of the discrete wavelet $g(t) = (1, -1, -2, 2, 1, -1)$, then

$Y = \{y_b\}$, $b = 0.....n(n = N + 1 - 6)$, is the wavelet transform of the signal given by:

$$S_{ab} = y_b = F_b^T X$$

where ^{T} indicates the transpose of the vector.

$$F_b = (\underbrace{0, ...0}_{b\times}, 1, -1, -2, 2, 1, -1, 0, ...0)^T;$$

In other words,

$$y_b = x_b - x_{b+1} - 2x_{b+2} + 2x_{b+3} + x_{b+4} - x_{b+5}$$

$$b = 0.....N + 1 - 6$$

Example:
$X = (0, 0, 0, 0, 0, 0, 0, 0, 0, 1, 1, 1, 1, 1, 1, 1)^T$:
a signal with a jump at the index i = 8, N = 14

The wavelet transform is :
$Y = (0, 0, 0, -1, 0, 2, 0, -1, 0, 0)^T$ (n=9).

The jump in the signal at the index i is detected in 3 points in the response signal Y at the index $j = i - 5$, $j = i - 3$ and $j = i - 1$ ($j = 3$, $j = 5$ and $j = 7$).

Only the occurrence of this sequence of 3 points allows to detect cycle slips out of the noise of the signal.
The values of the coefficients give information about the amplitude of the cycle slip.

Example of a result

The wavelet transform of the signal shown in Figure 7 using the wavelet given in Figure 5 is represented in Figure 8.
The presence of three outliers in the wavelet transform indicates the occurrence of a cycle slip.

3.2 Study of simulated jumps on theoretical and real GPS signals

We performed our study in three steps. We successively study:

- the capability of the wavelet transform to evaluate 'lost' data,
- the capability of the wavelet transform to evaluate jumps in the data,
- the capability of the wavelet transform to evaluate jumps in the data that occur after a gap in the data.

These tests were performed on three kinds of data:

- simulated data with white noise,
- real GPS signals in which artificial gaps and jumps are introduced,
- real GPS signals with real cycle slips.

3.2.1 Simulated data with white noise

First, the case of a parabola with white noise was considered.
Some data points were removed to test if the wavelet transform was able to recover these 'lost' points.
This simulation was accomplished for two reasons:

- if the sampling rate is, let's say 30 sec, is the wavelet transform able to compute an accurate predicted value after 60 sec, 90 sec, ... ?

- when a cycle slip occurs after a gap in the data, the reconstruction of the lost measurements is necessary for the evaluation of the cycle slip by the wavelet transform.

It is important to point out that the aim is not to 'build' data points but to evaluate the error on the calculation of a cycle slip occurring after a gap in the data.
In a second step, a jump was introduced in the parabola to evaluate the capability of the wavelet transform to detect and evaluate the jump. Finally, we introduced a jump after the gap in the data.
The wavelet transform passed these tests successfully: the accuracy of both recovered values and computed jumps was of the order of the noise introduced in the parabola.

3.2.2 Simulated gaps and jumps in real GPS data

The same three tests were carried out on Rogue data. A satellite pass was chosen where no jumps and no gaps were detected. The sample rate was 30 seconds. The work was accomplished with the phase combination PP which has to be used to compute the final cycle slip correction.

The results of the first test are presented in Table 1: we removed one to four data points at three different epochs in the satellite pass corresponding to different elevation angles and we tried to rebuild these removed values.
The first and the last epochs choosen (548010 and 570510) correspond to an elevation angle below 10 degrees, the other data points are above 30 degrees. It was important to consider low elevation angles in our work to study the limitations of this method as the signal to noise ratio of the GPS signal is much lower for low elevations. Consequently, the measurement noise is higher and the number of cycle slips is more important. In addition, the multipath effect is also more frequent in the case of low elevation angles. Table 1 shows that the accuracy of the restored values is of the order of the measurement noise. The accuracy of the recovered data depends of course on the number of 'lost' data.
Table 2 gives the results of the second and third tests where we introduced a jump of 1 cycle on L_1 and 1 cycle on L_2(1.1). Before this jump, a gap of zero to four data points was simulated. Again the accuracy of the computed jump is of the order of the measurement noise. The results obtained by Kalman filtering and the wavelet transform are of the same order. Obviously, the computed jumps are worse in the case of a low elevation angle. Other values than (1,1) for the cycle slip give the same results.

Table 1 and Table 2 display results for 4 missing data. No test has been made for larger gaps, but it is obvious that the more the measurement noise is important, the more it will be difficult to recover data and evaluate cycle slips after a large gap.

nb of rem.data	rem. epochs	obs-rebuilt	elev. < 10°
1	548010	−0.0383	⋆
	554400	−0.0001	
	570510	−0.0105	⋆
2	548010	−0.0155	⋆
	548040	0.0219	⋆
	554400	0.0018	
	554430	0.0026	
	570510	−0.0284	⋆
	570540	−0.0655	⋆
3	548010	−0.0154	⋆
	548040	0.0222	⋆
	548070	0.1359	⋆
	554400	0.0015	
	554430	0.0018	
	554460	0.0009	
	570510	−0.0087	⋆
	570540	−0.0261	⋆
	570570	−0.0060	⋆
4	548010	−0.0231	⋆
	548040	0.0068	⋆
	548070	0.1090	⋆
	548100	0.0412	⋆
	554400	−0.0002	
	554430	−0.0015	
	554460	−0.0049	
	554490	−0.0041	
	570510	−0.0119	⋆
	570540	−0.0327	⋆
	570570	−0.0175	⋆
	570600	−0.0247	⋆

Table 1: Reconstruction of removed observations using the modulus of the wavelet transform. Column 1 gives the number of removed data points. Column 2, the epochs (in GPS time) of removed observations and Column 3, the differences between the observed and the reconstructed values in cycles. A ⋆ appears in Column 4 when the removed data correspond to an elevation lower than 10 degrees.

C.S. epoch	C.S. L1	C.S. L2	number missing	WT difference	KF difference
548010 el = 9.2°	1	1	0	0.044	−0.003
			1	0.065	−0.055
			2	0.119	−0.136
			3	0.181	−0.283
			4	0.271	−0.392
551010 el = 29.1°	1	1	0	−0.016	0.005
			1	−0.027	0.012
			2	−0.024	0.035
			3	−0.040	0.061
			4	−0.080	−0.005
554400 el = 51.7°	1	1	0	−0.002	−0.001
			1	−0.001	−0.001
			2	−0.002	−0.004
			3	−0.006	−0.017
			4	−0.004	−0.016
562020 el = 67.0°	1	1	0	−0.009	−0.005
			1	−0.005	0.003
			2	0.008	0.020
			3	0.004	0.015
			4	−0.002	−0.013
570510 el = 9.4°	1	1	0	0.012	0.019
			1	−0.019	−0.046
			2	0.006	−0.037
			3	0.032	0.015
			4	0.086	0.092

Table 2: Evaluation of known jumps. Column 1 gives the epoch (in GPS seconds) at which a cycle slip has been added and the elevation (el) of the satellite at this epoch; Column 2 and Column 3 give (in cycles) the jumps added respectively on L1 and L2; Column 4 indicates the number of missing data points before the jump; Column 5 gives (in cycles) the difference between the jump added and the jump detected by the wavelet transform on the PP combination; Column 6 gives (in cycles) the results of the same test for the Kalman filter.

FILE data	S.V.#	epoch of cycle slip	elev	gap	Wavelet Transform PC_1	PC_2	PP	Kalman filter PC_1	PC_2	PP
1471.1	21	380310	9^0	90	6	−17	0.009	2	0	−0.315
1471.2	2	413790	12^0	60	−1	−2	0.077	−4	−1	−0.055
1481.2	17	446880	12^0	90	13	0	−0.076	1	−3	−0.126
1491.1	19	537030	13^0	60	−3	2	−0.036	0	0	−0.036
	26	530760	10^0	90	−7	15	0.065	−3	−2	−0.248
	31	537510	8^0	60	−7	9	0.026	0	0	0.096
1491.2	13	522630	24^0	120	1	1	−0.041	1	0	−0.039
	14	522720	19^0	210	3	−1	0.073	−3	−1	0.048
	19	522660	37^0	150	2	2	−0.044	1	0	0.065
	22	522660	10^0	60	0	0	−0.036	3	1	−0.021
	24	522660	45^0	150	0	−1	−0.012	−3	−2	0.062
	29	522660	39^0	150	0	0	0.014	0	0	−0.006

Table 3: Comparison of calculated residuals and 'real' residuals. In the first part of Table 3, Column 1 gives the name of the data file, Column 2, the satellite number, Column 3, the epoch of the cycle slip (in GPS seconds), Column 4, the satellite elevation, and Column 5, the duration (in seconds) of the gap in the data. The second part of this Table displays the results obtained by the wavelet transform (in cycles). It gives the difference between the "real" residual computed with the value of the cycle slip found by the double difference software and the residual computed by the wavelet transform (1) for the signal PC_1 (Column 1), (2) for the signal PC_2 (Column 2), and (3) the PP combination (Column 3). The third part of the Table contains the same information as part 2 concerning the results of the Kalman filter (in cycles).

3.3 Real cycle slips in GPS data

In 1993, the Royal Observatory of Belgium (ROB) has purchased four Turbo Rogue GPS receivers in order to participate in the IGS network and as support to deploy the national GPS geodetic network. This new receiver type is characterized by a very low measurement noise.

The results of the previous paragraph demonstrate clearly that the quality of the signal will play a very important role in the cycle slip correction.
In may 1993, two of these four receivers were continuously operating during three days on a 83 meters baseline in the park of the Observatory. The sampling interval was 30 seconds and the elevation mask 4 degrees.
First the cycle slips 'having no interest' were eliminated. For example, if a satellite pass begins with three data points followed by a gap of 2 minutes and finally uninterrupted measurements during several hours, the first three measurements are eliminated. Then a cycle slip repairing was attempted on the six data files using the wavelet transform, the Kalman filter and double differences computed by the self-written ROB-GPS software. Table 3 compares the differences between the first residuals (Observed - Predicted) on $PC1$, $PC2$ and PP computed by the wavelet transform and the Kalman filter and the 'correct' residuals computed with the value of the cycle slip found using the double differences. From a general point of vue, the Kalman filter gives better results in the PC_i modelisation: a Kalman filter with good a-priori values is well suited to describe a noisy signal.

On the other hand, the wavelet transform obtains better PP residuals. The two methods are thus very complementary.
These comments are less true for the file 1491.2 but in this case, the cycle slips occur above 19^o of elevation when the pseudorange noise is much lower.
To be sure to obtain a unique solution for the cycle slip, the accuracy of the PC_i residual has to be included in a $[-3,3]$ cycles interval around the correct cycle slip. In this case, the predicted PP residual has to be in a $[-0.14, 0.14]$ interval around the correct PP residual provided that a 1,1 or -1,-1 cycle slip gives a -0.28 or 0.28 jump in PP.
Table 3 shows that none of the two methods can realize these conditions in a hundred percent of the cases. This result explains why further development was necessary.

In the case of the Kalman filter the following solution was tried: the Kalman filter was applied on the data in the two directions (from the beginning to the end of file and from the end to the beginning) giving two residuals (one in each direction) for every test quantity (PC_1, PC_2, PP). The mean PC_i residual was computed when encountering a cycle slip. This supplementary step was not sufficient to guarantee a correct computation of the PP residual. Then an attempt was made to model the error in the PP value predicted by Kalman filtering in the two directions giving two more residuals.
The mean of these four PP residuals gave a value precise enough to obtain an unambiguous value for the cycle slip.

In the case of the wavelet transform method, the problem is solved as follows: the first cycle slip evaluation is used to correct the signals PC_1, PC_2 and PP giving the corrected signals PC_1^1, PC_2^1 and PP^1. The wavelet transform is then recomputed on the ionospheric free combination PP^1.
A new residual on PP^1 is found and is due to the error on the first evaluation of the cycle slips on PC_1 and PC_2. The first differences around the cycle slip in the corrected signals PC_1^1 and PC_2^1 are used to find the complementary correction to apply on PC_1^1 and PC_2^1. This complementary correction has to correspond with the new residual found on PP^1.
As a last verification, the wavelet transform is recomputed on the three signals : PC_1^2, PC_2^2 and PP^2. If there remains a jump, a new iteration is necessary.

When these supplementary steps were accomplished, both methods gave the correct cycle slip value.

4 Discussion and Conclusions

The aim of this paper was to demonstrate that the wavelet transform can be used to remove cycle slips in GPS measurements.
We showed that the method can evaluate missing data and correct simulated cycle slips even if they occur after a gap in the data. The accuracies achieved by the wavelet transform and the Kalman filter are of the same order.

The advantage of the wavelet transform method lies in the fact that the filter is easy to implement. It is very precise in the time location of a cycle slip and a response on 3 points makes the detection reliable.

The disadvantages of this method are 1) that the filter is a non-adaptative one, 2) a signal with a lot of noise can be seen as successive jumps.

The use of a Kalman filter requires a set of initial conditions: state vector, covariance matrix of the observations, state-transition noise matrix. The Kalman filter is very sensitive to these a priori values. Ideally, they should be adapted to the different situations that can be encountered: these values vary in function of the receiver type, the site (multipath), the ionospheric conditions,...
However, a suitable choice of these initial conditions will give a powerful tool to study a signal deteriorated by noise.

The wavelet transform does not need any a priori value, is very simple to implement but does not give as good results as the Kalman filter on noisy signals (i.e. the PC_i combination) but better results on the PP combination.

As presented in the previous section, The use of supplementary developments after obtaining the first residuals is necessary to find the exact cycle slip with each of the two methods.

As a consequence, the two mathematically independent methods seem to be very complementary and should be used together to give mutual confirmation of the computed cycle slips.

5 Acknowledgments

We should like to thank Prof. J-P. Antoine to have introduced us to the theory of wavelets. We are also grateful to P. Pâquet, B. Ducarme and C.Bruyninx for useful comments. K.Degryse and V.Dehant for their help in the English translation.

References

[1.] *Wavelets. Time-Frequency Methods and Phase Space (Proc. Marseille, Dec. 1987).*
J.-M. Combes, A. Grossmann, Ph. Tchamitchian (eds.). Berlin: Springer-Verlag, 1989, 2d ed., 1990.

A. Arnéodo, G. Grasseau, M. Holschneider,
Wavelet analysis of multifractals,
Phys. Rev. Lett. 61, pp. 2281-2284, 1988.

L. Bastos, H. Landau,
Fixing cycle slips in dual frequency kinematic GPS applications using Kalman filtering,
Manuscripta Geodetica, 13, pp. 249-256, 1988.

A. Bijaoui, M. Giudicelli,
Optimal image addition using the wavelet transform,
Experimental Astronomy, 1, pp. 347-363, 1991.

CH. K. Chui,
An Introduction to Wavelets,
Academic Press, 264 pp., 1992.

I. Daubechies,
Ten Lectures on Wavelets,
SIAM, 357 pp., 1992.

I. Daubechies,
Orthonormal bases of wavelets with finite support - Connection with discrete filters,
in [1.], pp. 38-67.

N. Delprat, B. Escudié, Ph. Guillemain, R. Kronland-Martinet, Ph. Tchamitchian, B. Torrésani,
Asymptotic wavelet and Gabor analysis: Extraction of Instantaneous frequencies,
IEEE transactions on Information Theory, 38, 2, pp.644-664, 1992.

H.J. Eueler and C. Goad,
On optimal filtering of GPS dual frequency observations without using orbit information,
Bulletin géodésique, 65 pp. 130-143, 1991.

A. Grossmann, J. Morlet, T. Paul,
Transforms associated to square integrable group representation I.General results,
J. Math. Phys., 26, pp. 2473-2479, 1985.

A. Grossmann, Ph. Guillemain, R. Kronland-Martinet,
Arête associée à la transformée en ondelettes de signaux présentant des singularités isolées,
Proceedings of the International conference on 'Wavelets and Applications', Toulouse, 1992, to be published.

P. Guillemain, R. Kronland-Martinet, B. Martens.
"Application de la transformée en ondelettes en spectroscopie RMN".
rapport CNRS-LMA (Marseille), No112, 1989.

Ph. Guillemain, R. Kronland-Martinet,
Parameters estimation through continuous wavelet transform for synthesis of audio-sounds,
an audio engineering society, prepint 1991.

M. Holschneider, R. Kronland-Martinet, J. Morlet, Ph. Tchamitchian,
A real-time algorithm for signal analysis with the help of the wavelet transform.
in [1.], pp. 286-297.

R.W. King, EG Masters, C.Rizos, A.Stolz and J.Collins,
Surveying with Global Positioning System,
Dümmler, Bonn, 1987.

H. Landau,
Precise kinematic GPS positioning: Experiences on a Land Vehicule using TI 4100 receivers and software,
Bulletin géodésique, 63, pp. 85-96, 1989.

H. Lichtenegger, B. Hoffmann-Wellenhof,
GPS data preprocessing for cycle slip detection,
Paper presented at the 125th Anniversary General Meeting of IAG, Edinburgh, 1989.

B. Martens,
"Application de l'analyse en ondelettes à la RMN".
Mémoire de Licence, UCL, Louvain-la-Neuve, 1989.

Y. Meyer,
"Ondelettes : Algorithmes et applications"
Ed. Armand Colin, 184 pp., 1992.

E. Slezak, A. Bijaoui, G. Mars,
Identification of structures from galazy counts: use of the wavelet transform,
Astron. Astrophys., 227, pp. 301-316, 1990.

B. Torrésani,
Un logiciel d'analyse en ondelettes par l'agorithme a trous,
Rapport no3, Centre de Physique théorique CNRS-Luminy, 1988.